RECENT RESULTS ON DIRECT CP VIOLATION FROM NA48 EXPERIMENT AT CERN

A. BIZZETI[1,2]

REPRESENTING THE NA48 COLLABORATION:

Cagliari, Cambridge, CERN, Dubna, Edinburgh, Ferrara, Firenze, Mainz,
Orsay, Perugia, Pisa, Saclay, Siegen, Torino, Vienna, Warsaw

[1]*Dipartimento di Fisica dell'Università di Modena e Reggio Emilia, Modena, Italy*
[2]*I.N.F.N., Sezione di Firenze, Sesto Fiorentino, Italy*

The direct CP violation parameter $\mathrm{Re}(\varepsilon'/\varepsilon)$ has been measured from two-pion decays of neutral kaons by the NA48 experiment at CERN SPS. The analysis of a new data sample, collected in 2001 under different conditions compared to earlier years (1997–99), provide the result: $\mathrm{Re}(\varepsilon'/\varepsilon) = (13.7 \pm 3.1) \times 10^{-4}$. Combining this result with that published from 1997–98-99 data, we obtain an overall value $\mathrm{Re}(\varepsilon'/\varepsilon) = (14.7 \pm 2.2) \times 10^{-4}$ from the NA48 experiment.

1 Introduction

CP violation was discovered in the neutral kaon system in 1964 [1] with the first observation of the CP-forbidden decay $K_L \to \pi^+\pi^-$. If CP were conserved, $\mathrm{K_S}$ and $\mathrm{K_L}$ particles would be pure CP eigenstates, decaying only into $CP = +1$ and $CP = -1$ final states, respectively. The observation of $K_L \to 2\pi$ ($CP = +1$) decays provides a clear evidence of CP non conservation.

The main component of CP violation is due to the mixing of the CP eigenstates, called *indirect* CP violation and represented by the mixing parameter ε. Another component, called *direct* CP violation and represented by the parameter ε', may originate in the decay process through the interference of amplitudes with different isospins.

In the Standard Model of electro-weak interactions, CP violation originates from an irreducible complex phase in the quark mixing matrix [2].

Current theoretical predictions of ε'/ε range from $\approx -10 \times 10^{-4}$ to $\approx +40 \times 10^{-4}$ [3].

The direct CP violation component is determined by measuring the double ratio R of partial decay widths, which is related to ε'/ε as follows[1]:

$$R \equiv \frac{\Gamma(\mathrm{K_L} \to \pi^0\pi^0)/\Gamma(\mathrm{K_S} \to \pi^0\pi^0)}{\Gamma(\mathrm{K_L} \to \pi^+\pi^-)/\Gamma(\mathrm{K_S} \to \pi^+\pi^-)} \simeq 1 - 6\,\mathrm{Re}(\varepsilon'/\varepsilon) \qquad (1)$$

Results on direct CP violation were published by two experiments in 1993: NA31 [4] measured $\mathrm{Re}(\varepsilon'/\varepsilon) = (23.0 \pm 6.5) \times 10^{-4}$, while E731 [5] measured $\mathrm{Re}(\varepsilon'/\varepsilon) = (7.4 \pm 5.9) \times 10^{-4}$.

More recently, NA48 published the measurement [6] $\mathrm{Re}(\varepsilon'/\varepsilon) = (15.3 \pm 2.6) \times 10^{-4}$, obtained from the analysis of data collected in 1997 [7], 1998 and 99, and KTeV presented a preliminary value [8] $\mathrm{Re}(\varepsilon'/\varepsilon) = (20.7 \pm 2.8) \times 10^{-4}$ from data accumulated in 1996 [9] and 1997. These results provide a convincing evidence of direct CP violation in the decay of neutral kaons.

We report here a measurement of $\mathrm{Re}(\varepsilon'/\varepsilon)$ performed by NA48 using the 2001 data sample, recorded in different experimental conditions compared to earlier years. The main differences consist in the drift chambers, rebuilt after the implosion of the beam tube in november 1999, and the SPS beam. Thanks to an extended SPS duty cycle, made possible after the closure of LEP, data were taken at a 30% lower instantaneous beam intensity while keeping about the same per day statistics.

The 2001 data, equivalent to roughly half of the total 1998+99 statistics, have been used to check the insensitivity of the result to intensity-related effects and to complete the statistics for the final $\mathrm{Re}(\varepsilon'/\varepsilon)$ measurement.

2 The NA48 method

The double ratio R, from which $\mathrm{Re}(\varepsilon'/\varepsilon)$ is derived, is measured by counting the number of decays in each of the four decay modes. The experiment is designed to obtain cancellation of systematic effects contributing symmetrically to different components of the double ratio.

[1] as the phase of ε' and that of $\varepsilon(\simeq -\pi/4)$ are very close, we get $\varepsilon'/\varepsilon \simeq \mathrm{Re}(\varepsilon'/\varepsilon)$.

The sensitivity of the measurement to accidental activity and to variations in beam intensity and detection efficiency is minimized by the simultaneous collection of the four decay modes in the same decay region. Dead time conditions affecting any of the decay modes are recorded and applied offline to all modes. In order to eliminate the effect of the small and slow variations of the $\mathrm{K_L}$ and $\mathrm{K_S}$ beam intensities, $\mathrm{K_S}$ events are further weighted by the $\mathrm{K_L}/\mathrm{K_S}$ intensity ratio.

Two nearly-collinear neutral beams, converging to the center of the electromagnetic calorimeter, provide $\mathrm{K_L}$ and $\mathrm{K_S}$ decays in the same fiducial region with similar momentum spectra. In order to be insensitive to residual differences in the beam momentum spectra, the analysis is performed in bins of kaon energy.

The difference between $\mathrm{K_L}$ and $\mathrm{K_S}$ acceptances, due to different mean decay lengths, is minimized by weighting the $\mathrm{K_L}$ decays as a function of their proper lifetime, such that the $\mathrm{K_L}$ decay distribution becomes similar to the $\mathrm{K_S}$ one. The small remaining differences in beam divergences and geometries are taken into account using a Monte Carlo simulation.

Decays from the $\mathrm{K_S}$ beam are identified by a coincidence between the decay time and the registered times of the protons producing the $\mathrm{K_S}$ beam.

Residual backgrounds which do not cancel in the double ratio are minimized by identifying the $\pi^+\pi^-$ and $\pi^0\pi^0$ decays with high-resolution detectors.

A detailed description of the NA48 experimental apparatus and of the analysis of 1998–99 data can be found in [6].

3 Beams, detectors and triggers

The NA48 $\mathrm{K_L}$ and $\mathrm{K_S}$ simultaneous beams [10] are produced in two different targets by 400 GeV/c protons from the same SPS beam, having a cycle time of 16.8 s and a spill length of 5.2 s.[2] The ratio of their intensities is stable within 10%. The $\mathrm{K_L}$ beam intensity in 2001, measured from the number of selected $\mathrm{K_L}$ decays as a function of time within the extraction, is shown in Fig. 1 together with the intensity measured on 1999 data.

[2] The beam momentum was 450 GeV/c, the cycle time 14.4 s and the spill length 2.4 s in the 1997, 1998 and 1999 runs.

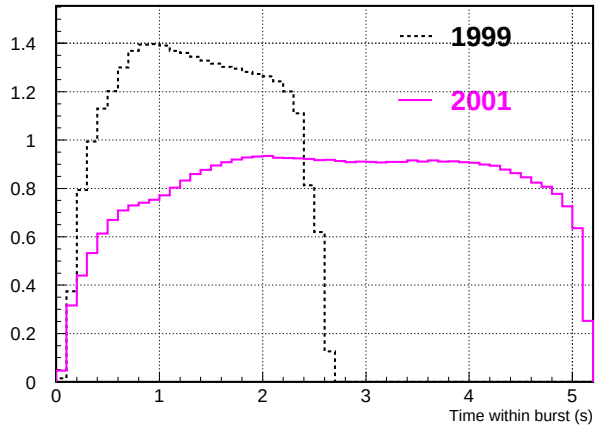

Figure 1: Rate of selected $\mathrm{K_L}$ events along the proton burst (in 0.1 s bins), proportional to the $\mathrm{K_L}$ beam intensity, in 2001 and 1999 data taking periods.

An array of scintillators [11] (Tagger) is used to record the time of protons producing the $\mathrm{K_S}$ beam. An anti-counter [12] (AKS), formed by a photon converter and three scintillation counters is located on the $\mathrm{K_S}$ beam at the beginning of the decay region.

Charged particles are measured by a magnetic spectrometer [13], consisting of a dipole magnet giving a momentum kick of 265 MeV/c and four drift chambers, with a momentum resolution $\sigma_p/p = 0.48\% \oplus 0.009\% \times p/(1\ \mathrm{GeV/c})$. A scintillator hodoscope composed of two planes of orthogonal strips is located after the spectrometer to provide a precise time measurement for charged particles. The signals from hodoscope strips are combined in four quadrants by a fast logic electronics for the first level of the $\pi^+\pi^-$ trigger.

The energy, impact point and arrival time of photons from $\pi^0\pi^0$ events are measured by a quasi-homogeneous liquid kripton (LKr) electromagnetic calorimeter [14] with a projective tower read-out. The energy resolution is $\sigma_E/E = 3.2\%/\sqrt{E} \oplus 9\%/E \oplus 0.42\%$ (E in GeV), the spatial resolution better than 1 mm above 25 GeV.

An iron-scintillator hadron calorimeter is located downstream of the electromagnetic calorimeter, followed by a muon counter made of three planes of scintillator separated by 80 cm thick iron walls.

The beam intensities are measured by two beam counters, one of

which ($\mathrm{K_L}$ monitor) located at the end of the beam line, the other ($\mathrm{K_S}$ monitor) near the target originating the $\mathrm{K_S}$ beam. Additional high-rate beam monitors have been installed before the 2001 run, the one for the $\mathrm{K_S}$ beam located near the Tagger, allowing to measure beam structures down to ≈ 200 ns.

About 4×10^5 particles per second reach the NA48 detectors. The trigger system is designed to reduce this rate to less than 10 kHz, with minimal loss from dead time and inefficiencies. The small inefficiencies of the main ($\pi^+\pi^-$ and $\pi^0\pi^0$) triggers are directly measured using data selected by redundant low-bias triggers. Other triggers, initiated by the beam monitors, are used to record the accidental activity with rates proportional to the $\mathrm{K_L}$ and $\mathrm{K_S}$ beam intensities.

The trigger for $\pi^0\pi^0$ decays [15] makes use of the vertical and horizontal projections of the LKr calorimeter to reconstruct the total deposited energy, the longitudinal decay position and the extrapolated kaon impact point.

A two-level trigger system is used for the $\pi^+\pi^-$ events. The first level reduces the rate to about 100 kHz using a coincidence of three fast signals: opposite quadrant coincidence in the scintillator hodoscope, hit multiplicity in the first drift chamber and total calorimetric energy above a threshold of 35 GeV. At the second level [16], a farm of asynchronous microprocessors performs a fast event reconstruction using data from the drift chambers and selects events compatible with a $K \to \pi^+\pi^-$ decay.

4 Data analysis

4.1 Event selection

The $K \to \pi^0\pi^0$ events are selected requiring four in-time photons detected by the electromagnetic calorimeter. From their measured energies and impact points, the decay vertex position along the beam axis is reconstructed imposing that the four-photon invariant mass corresponds to the kaon mass. The invariant masses of the two photon pairs are then computed (with resolution better than 1 MeV/c^2) and a χ^2 variable for the $\pi^0\pi^0$ hypothesis is calculated. A cut is applied on this variable in order to reject the residual background from $\mathrm{K_L} \to 3\pi^0$ events.

The $K \to \pi^+\pi^-$ events are selected using informations from the spectrometer. Both the longitudinal and transverse positions of the decay vertex can be determined, with resolutions of about 50 cm and 0.2 cm, respectively. Since the beams are vertically separated by about 6 cm in the decay region, a clean identification of the $\mathrm{K_S}$ and $\mathrm{K_L}$ decays is therefore possible using the reconstructed vertex position. A cut is applied on the asymmetry $\mathcal{A} = |p_1 - p_2|/(p_1 + p_2)$ between the two tracks momenta in order to remove asymmetric decays in which one of the tracks could be close to the beam pipe, where the Monte Carlo modelling is more difficult. Backgrounds from $\Lambda \to p\pi^-$ and $\bar{\Lambda} \to \bar{p}\pi^+$ are almost completely eliminated by this cut.

Background from semileptonic $\mathrm{K_L}$ decays is strongly suppressed by rejecting events with a track consistent with being either an electron or a muon. Electrons are rejected by requiring the ratio E/p of the energy deposited by the track in the LKr calorimeter over the track momentum to be less than 0.8. Muons are rejected by requiring no in-time hits in the muon counters near the track impact point. A further background suppression is achieved by applying kinematic cuts on the two-pion invariant mass $m_{\pi\pi}$ and on the kaon transverse momentum p'_T.

4.2 $\mathrm{K_S}$ tagging

A decay is labeled $\mathrm{K_S}$ if a coincidence is found (within a ± 2 ns time interval) between the event time and a proton time measured by the Tagger; otherwise the decay is labeled $\mathrm{K_L}$.

The time distributions for kaon decays to $\pi^+\pi^-$ final states, identified as $\mathrm{K_S}$ or $\mathrm{K_L}$ by their vertex position, is shown in Fig. 2. As tagging is the only available way to distinguish $\mathrm{K_S}$ from $\mathrm{K_L}$ in $\pi^0\pi^0$ decays, this method is used for both $\pi^0\pi^0$ and $\pi^+\pi^-$ modes. The double ratio is therefore sensitive only to differences in misidentification probabilities between the two decay modes and not to their absolute values, so that systematic effects are mostly symmetric.

The probability α_{S_L} that, due to coincidence inefficiencies, a $\mathrm{K_S}$ decay is identified as a $\mathrm{K_L}$, is called *tagging inefficiency*. In the $\pi^+\pi^-$ mode it is directly measured (using the vertical vertex position) to be $\alpha_{S_L}^{+-} = (1.12 \pm 0.03) \times 10^{-4}$ and is found to be dominated by the Tagger inefficiency.

The difference between the tagging inefficiencies in $\pi^+\pi^-$ and $\pi^0\pi^0$ decays is estimated by comparing the time measurements obtained from

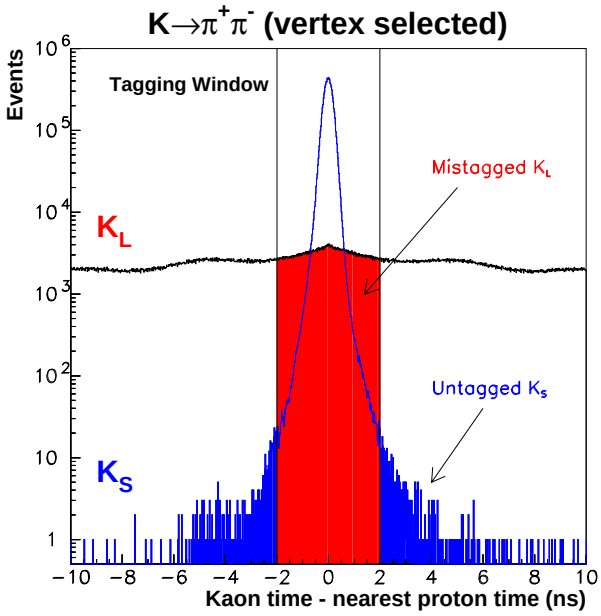

Figure 2: Time coincidence with nearest proton in the Tagger, for $\mathrm{K_S}$ and $\mathrm{K_L}$ decays to $\pi^+\pi^-$ identified by their reconstructed vertex.

the LKr calorimeter and from the scintillator hodoscope in $2\pi^0$ and $3\pi^0$ events where one of the photons converts into an electron-positron pair.

The $\pi^0\pi^0$ and $\pi^+\pi^-$ tagging inefficiencies agree within an uncertainty of $\pm 0.5 \times 10^{-4}$, corresponding to an uncertainty on R of $\pm 3 \times 10^{-4}$.

The probability α_{LS} that, due to an accidental coincidence between the event and a proton, a $\mathrm{K_L}$ decay is identified as a $\mathrm{K_S}$, is called *accidental tagging*. It is measured in the $\pi^+\pi^-$ mode and results to be[3] $\alpha_{LS}^{+-} = (8.115 \pm 0.010) \times 10^{-2}$.

The difference $\Delta\alpha_{LS}$ between the α_{LS} values in $\pi^0\pi^0$ and $\pi^+\pi^-$ decays is determined by measuring the probability to find a proton within time windows 4 ns wide, located before or after the event time in $\mathrm{K_L}$ events.

The resulting value of $\Delta\alpha_{LS} \equiv \alpha_{LS}^{00} - \alpha_{LS}^{+-} = (+3.4 \pm 1.4) \times 10^{-4}$ corre-

[3] It was $(10.649 \pm 0.008) \times 10^{-2}$ in the 1998–99 data sample.

sponds to a correction on R of $(+6.9 \pm 2.8) \times 10^{-4}$.

4.3 Definition of the decay region

Events are counted within the following fiducial ranges in kaon energy E_K and proper time τ: $70\ \mathrm{GeV} < E_K < 170\ \mathrm{GeV}$; $0 < \tau < 3.5\tau_S$, where $\tau = 0$ corresponds to the position of the AKS counter and τ_S is the $\mathrm{K_S}$ lifetime. For $\mathrm{K_L}$ decays, the proper time cut is applied on the reconstructed τ, while for $\mathrm{K_S}$ the lower cut is applied using the AKS to veto decays occurring upstream. The nominal $\tau = 0$ position defined by the AKS differ by 21.0 ± 0.5 mm between $\pi^+\pi^-$ and $\pi^0\pi^0$ decays, resulting in a correction on R of $(+1.2 \pm 0.3) \times 10^{-4}$.

$\mathrm{K_S} \to \pi\pi$ decays can be produced in both beams by scattering of beam particles in the collimators and, in the $\mathrm{K_S}$ case, in the AKS counter. To reduce this contamination, the extrapolated kaon impact point on the LKr calorimeter is required to be within 10 cm of the intersecting beam axes.

5 Calculation of R and systematic uncertainties

The calculation of R is performed dividing the data into 20 bins in kaon energy, each bin 5 GeV wide. The numbers of $\mathrm{K_S}$ and $\mathrm{K_L}$ candidates, corrected for the mistagging probabilities, are shown in Table 1.

Table 1

Number of events (corrected for mistagging).		
	$\to \pi^0\pi^0$	$\to \pi^+\pi^-$
$\mathrm{K_L}$	1.546×10^6	7.136×10^6
$\mathrm{K_S}$	2.159×10^6	9.605×10^6

Corrections for trigger inefficiencies, background subtraction, and residual acceptance differences between $\mathrm{K_S}$ and $\mathrm{K_L}$ are applied separately in each energy bin before computing the average of R.

Corrections and systematic uncertainties from mistagging and AKS have already been discussed in the previous Section.

5.1 Trigger efficiencies

Events triggered by a scintillating fiber detector located inside the LKr calorimeter have been used to measure the $\pi^0\pi^0$ trigger efficiency, which results to be $(99.901 \pm 0.015)\%$. As this efficiency is $\mathrm{K_S} - \mathrm{K_L}$ symmetric, no correction to the double ratio needs to be applied.

$(98.697 \pm 0.017)\%$. The difference in this efficiency between $\mathrm{K_S}$ and $\mathrm{K_L}$ decays is computed in each energy bin, and the overall correction to the double ratio results to be $(+5.2 \pm 3.6) \times 10^{-4}$, where the uncertainty is given by the statistics of the control samples used to measure the efficiency.

5.2 Backgrounds

The only background affecting the $\mathrm{K_L} \to \pi^0\pi^0$ data comes from $\mathrm{K_L} \to 3\pi^0$ decays, while the $\mathrm{K_S}$ mode is background free. The $\mathrm{K_L} \to 3\pi^0$ background, uniformly distributed in the χ^2 variable, is estimated using a control region in the χ^2 distribution. The excess of $\mathrm{K_L}$ candidates in this region over a Monte Carlo expectation for $\pi^0\pi^0$ decays is used to extrapolate the background in the signal region. Background subtraction is performed in kaon energy bins; the overall correction to the double ratio is $(-5.6 \pm 2.0) \times 10^{-4}$.

Two control regions in the $m_{\pi\pi} - {p'_T}^2$ plane are used to estimate the residual K_{e3} and $K_{\mu 3}$ backgrounds in the $\mathrm{K_L} \to \pi^+\pi^-$ sample. The background distributions in these control regions are modelled by a K_{e3} sample, selected with $(E/p)_e > 0.95$, and by a $K_{\mu 3}$ sample, obtained by reversing the muon veto requirement. The tails in the $\mathrm{K_L} \to \pi^+\pi^-$ distribution are estimated from the $\mathrm{K_S}$ sample. The result is then extrapolated to the signal region, obtaining for the K_{e3} and $K_{\mu 3}$ background fractions the values 10.5×10^{-4} and 3.0×10^{-4}, respectively. These backgrounds are subtracted in kaon energy bins, resulting in a correction to R of $(+14.2 \pm 3.0) \times 10^{-4}$.

In the $\mathrm{K_S}$ beam, the cut on the extrapolated kaon impact point is stronger than the ${p'_T}^2$ cut applied to the $\pi^+\pi^-$ events. As a consequence, beam scattering events are removed in the same way from both $\pi^0\pi^0$ and $\pi^+\pi^-$ samples. On the contrary, in the $\mathrm{K_L}$ beam the ${p'_T}^2$ cut applied only to the $\pi^+\pi^-$ events is stronger, therefore a small residual contribution from scattering is left only in the $\pi^0\pi^0$ sample. The correction for this effect is determined using $\mathrm{K_L} \to \pi^+\pi^-$ candidates with an inverted ${p'_T}^2$

cut and applied in kaon energy bins. The resulting overall correction to the double ratio is $(-8.8 \pm 2.0) \times 10^{-4}$.

5.3 Acceptance

The difference between $\mathrm{K_S}$ and $\mathrm{K_L}$ acceptances is minimized (in both decay modes) by weighting $\mathrm{K_L}$ events according to their proper decay time.

The small residual difference, due to the different beam sizes and directions, is computed using a large-statistics Monte Carlo simulation (4×10^8 generated kaon decays per mode). The resulting correction to R is $(+21.9 \pm 3.5_{\mathrm{MCstat}} \pm 4.0_{\mathrm{syst}}) \times 10^{-4}$.

5.4 Event reconstruction

Kaon energy, decay vertex and proper time in the $\pi^0\pi^0$ events are determined using the photon energies and positions measured with the LKr calorimeter. The absolute energy scale is fixed using $\mathrm{K_S} \to \pi^0\pi^0$ events and the known position of the AKL counter. Special runs (so-called η runs) with a π^- beam striking two thin targets located near the beginning and the end of the fiducial decay region have been used to cross-check the energy scale with two-photon decays of prompt π^0 and η mesons.

Linearity and spatial uniformity in the energy response are studied using K_{e3} decays, where the electron energy measured with the calorimeter can be compared to the momentum measured with the spectrometer, and using data from η runs. Position measurements with the calorimeter are also checked using K_{e3} data.

The total systematic error on the double ratio from the measurement of the photon energies and positions results to be $\pm 5.3 \times 10^{-4}$.

The uncertainty on R from the reconstruction of $\pi^+\pi^-$ decays, due to uncertainties in the detector geometry, is estimated to be $\pm 2.8 \times 10^{-4}$.

5.5 Intensity effects

The accidental activity in NA48 detectors is mainly produced by kaon decays in the high-intensity $\mathrm{K_L}$ beam. The overlap of extra particles with a good event may result in the loss of the event at the trigger or

data analysis level. The effect on R is minimized by the simultaneous collection of the four decay modes and by the fact that $\mathrm{K_S}$ and weighted $\mathrm{K_L}$ decays illuminate the detector in a similar way.

The possible residual effect can be separated into two components. The first one (intensity difference) is caused by intensity variations between the two beams coupled to different, intensity-dependent, event losses in the $\pi^+\pi^-$ and $\pi^0\pi^0$ modes. The other one (illumination difference) originates from a residual difference in the illumination between $\mathrm{K_S}$ and $\mathrm{K_L}$ decays coupled to a dependence of the event loss probability on the impact points of the kaon decay products.

Assuming a linear dependence of the event loss probability on the $\mathrm{K_L}$ beam intensity, the intensity difference effect is given by $\Delta R = \Delta\lambda \times \Delta I/I$, where $\Delta\lambda$ is the difference between the mean losses in $\pi^+\pi^-$ and $\pi^0\pi^0$ modes and $\Delta I/I$ is the relative difference between the average $\mathrm{K_L}$ beam intensity as seen by $\mathrm{K_L}$ and $\mathrm{K_S}$ events. The latter is measured in different ways: from detector activity within the readout time window before the event, from $\mathrm{K_L}$ beam monitor counts integrated over a 200 ns time window and from the correlation between $\mathrm{K_S}$ and $\mathrm{K_L}$ beams, computed using beam monitor counts taken at regular times during beam extraction. All methods agree with a zero result within a $\pm 1\%$ uncertainty.

$\Delta\lambda$ is estimated by overlaying data and Monte Carlo events with events taken with the beam monitor trigger, and is found to be $(1.0 \pm 0.5) \times 10^{-2}$, with a linear dependence on the beam intensity, as expected. The uncertainty on R from the intensity difference effects results to be $\pm 1.1 \times 10^{-4}$, significantly better than in 1998–99 data due to the lower beam intensity and improved beam monitors.

The illumination difference effect is also estimated using the overlay technique. The corresponding uncertainty on the double ratio is evaluated to be $\pm 3.0 \times 10^{-4}$.

The effects of additional "in-time" detector activity, generated by the same collision in the $\mathrm{K_S}$ target producing the $\mathrm{K_S}$ event, are not taken into account by the methods described above. These effects have been studied mainly by searching, in $\pi^0\pi^0$ events from pure $\mathrm{K_S}$ beam runs, for additional energy clusters in the LKr calorimeter. The effect on R is less than 1×10^{-4}.

6 Results

A summary of the corrections applied to R and of the systematic uncertainties on the double ratio is shown in table 2, together with the corresponding values obtained in the analysis of 1998–99 data [6].

Table 2

Corrections and systematic uncertainties on R, in 10^{-4} units			
	2001	1998–99	
$\pi^+\pi^-$ trigger inefficiency	5.2 ± 3.6	-3.6 ± 5.2	(stat)
AKS inefficiency	1.2 ± 0.3	1.1 ± 0.4	
Reconstruction of $\pi^+\pi^-$	± 2.8	2.0 ± 2.8	
Reconstruction of $\pi^0\pi^0$	± 5.3	± 5.8	
Background to $\pi^+\pi^-$	14.2 ± 3.0	16.9 ± 3.0	
Background to $\pi^0\pi^0$	-5.6 ± 2.0	-5.9 ± 2.0	
Beam scattering	-8.8 ± 2.0	-9.6 ± 2.0	
Accidental tagging	6.9 ± 2.8	8.3 ± 3.4	(stat)
Tagging inefficiency	± 3.0	± 3.0	
Acceptance (statistical)	21.9 ± 3.5	26.7 ± 4.1	(stat)
(systematic)	± 4.0	± 4.0	
Accidental activity:			
intensity difference	± 1.1	± 3.0	
illumination difference	± 3.0	± 3.0	(stat)
K_S in time activity	± 1.0	± 1.0	
Total	+35.0 ± 6.5	$+35.9 \pm 8.1$	(stat)
	± 9.0	± 9.6	

The residual acceptance correction is mostly due to beam geometry effects and is well evaluated by Monte Carlo simulation. Some systematic uncertainties (indicated with "stat" in Table 2) are determined by the statistical significance of the control sample used.

The final result from 2001 data is $R = 0.99181 \pm 0.00147_{\rm stat} \pm 0.00110_{\rm syst}$, corresponding to $\mathrm{Re}(\varepsilon'/\varepsilon) = (13.7 \pm 2.5_{\rm stat} \pm 1.8_{\rm syst}) \times 10^{-4}$. This result is in good agreement with the published value $\mathrm{Re}(\varepsilon'/\varepsilon) = (15.3 \pm 2.6) \times 10^{-4}$, obtained from 1997–98-99 data at a different average beam intensity. Taking into account the correlated systematic uncertainty of $\pm 1.4 \times 10^{-4}$, the combined final result from the NA48 experiment is $\mathrm{Re}(\varepsilon'/\varepsilon) = (14.7 \pm 2.2) \times 10^{-4}$.

References

[1] J.H. Christenson et al., Phys. Rev. Lett. **13** (1964) 138.

[2] M. Kobayashi and K. Maskawa, Prog. Theor. Phys. **49** (1973) 652.

[3] M. Ciuchini, G. Martinelli, Nucl. Phys. **B** (Proc. Suppl.) **99B** (2001) 27;
E. Pallante et al., Nucl. Phys. **B 617** (2001) 441;
A.J. Buras et al., Nucl. Phys. **B 592** (2001) 55;
S. Bertolini et al., Phys. Rev. **D 63** (2001) 056009;
Y.L. Wu, Phys. Rev. **D 64** (2001) 0106001;
J. Donoghue, in: F. Costantini et al. (Eds), Proc. Int. Conf. on Kaon Physics Frascati Physics Serie **26** (2001) p. 93;
T. Hambye et al., Nucl. Phys. **B 564** (2000) 391;
J. Bijnens and J. Prades, JHEP **0006** (2000) 035;
T. Blum et al., hep-lat/0108013;
J.I. Noaki et al., hep-lat/0110075.

[4] G. Barr et al., Phys. Lett. **B 317** (1993) 233.

[5] L.K. Gibbons et al., Phys. Rev. Lett. **70** (1993) 1203.

[6] A. Lai et al., Eur. Phys. J. **C 22** (2001) 231–254.

[7] V. Fanti et al., Phys. Lett. **B 465** (1999) 335–348.

[8] A. Glazov, KTeV Collaboration, in: F. Costantini et al. (Eds.), Proc. Int. Conf. on Kaon Physics Frascati Physics Serie **26** (2001) p. 115.

[9] A. Alavi-Harati et al., Phys. Rev. Lett. **83** (1999) 22.

[10] C. Biino et al., CERN-SL-98-033(EA) and in: S. Myers, L. Liljeby and C. Petit-Jean-Genaz (Eds), Proc. 6th EPAC, IOP, Bristol, 1999.

[11] P. Grafström et al., Nucl. Instr. Meth. **A 344** (1994) 487;
H. Bergauer et al., Nucl. Instr. Meth. **A 419** (1998) 623.

[12] R. Moore et al., Nucl. Instr. Meth. **B 119** (1996) 149.

[13] D. Béderède et al., Nucl. Instr. Meth. **A 367** (1995) 88;
I. Augustin et al., Nucl. Instr. Meth. **A 403** (1998) 472.

[14] G.D. Barr et al., Nucl. Instr. Meth. **A 370** (1993) 413.

[15] G. Barr et al., Nucl. Instr. Meth. **A 485** (2002) 676.

[16] S. Anvar et al., Nucl. Instr. Meth. **A 419** (1998) 686.